Effect of selective nanopatterns on the performance of a pentacene-based thin-film transistor

Chang-Jae Yu,[1] You-Jin Lee,[1] Jong Sun Choi,[2] and Jae-Hoon Kim[1,a)]

[1]*Department of Electronic Engineering, Hanyang University, Seoul 133-791, Republic of Korea*
[2]*School of Electronic and Electrical Engineering, Hongik University, Seoul 121-791, Republic of Korea*

We investigate an effect of selective nanopatterns on the performances of a pentacene-based organic thin-film transistor (OTFT) in a top contact configuration. The one-dimensional nanopatterns onto an insulating layer are selectively formed at the channel and/or the source/drain (S/D) regions using the electron-beam lithography. The performance of the S/D-patterned OTFT was greater than that of the patternless OTFT while the performance of the channel-patterned OTFT was rather less. From Fowler–Nordheim analysis, it is found that the mobility improvement in the nanopatterned OTFTs is mainly originated from the enhanced carrier injection by the nanopatterns at the S/D regions rather than the enhancement of the current flow in the channel region. © *2011 American Institute of Physics.* [doi:10.1063/1.3598422]

Organic thin-film transistors (OTFTs) have been studied extensively for plastic electronic applications[1–3] including display driving elements[4,5] and electronic logic elements[6] due to the mechanical flexibility and low temperature processibility. It has been believed that the field-effect mobility, which is one of the most important factors dictating the electrical performances of the OTFTs, strongly relies upon the interfacial interactions of an organic semiconductor with a gate insulator and metal electrodes. Various methods to manipulate the interface with insulating layer[7–9] and/or a metal electrode[10–13] have been investigated to improve the OTFT performances. It was reported that the photo- or the thermal-treatment of organic insulator enhanced carrier mobility due to the structural ordering of the pentacene molecules on the treated insulators.[7,8] Recently, it has been demonstrated that the in-plane ordering of the pentacene molecules on a groove-patterned insulator enhances the mobility of the OTFT and gives rise to the mobility anisotropy.[9,14] However, most of studies just focused on the ordering of organic semiconductor not on other parameters like how to influence the nanopatterns on the charge injection at the interface with metal electrode.

In this letter, we investigate the effect of the nanopatterns on the OTFT performances through the selective patterns onto the insulating layer, source/drain (S/D) region, channel region between S/D, or whole regions. It was known that the mobility enhancement in the insulator-patterned OTFTs, where the patterns were formed in both channel and S/D regions, was mainly originated from the improvement of the current flow in the channel region.[9,14] In our investigations for the selectively patterned OTFTs, the performance of the S/D-patterned OTFT is greater than that of the reference OTFT without the nanopattern. Furthermore, it is better than that of the wholly patterned OTFT at the channel and S/D regions. From the Fowler–Nordheim (FN) anaylsis[15] of the current characteristics in a metal/semiconductor/metal (MSM) structure, it is found that the reduction in an injection barrier by the nanopatterns at the S/D regions gives rise to

the enhancement of the carrier injection and thus the mobility is remarkably improved in the pentacene-based OTFTs. Finally, we conclude that the device performances of the insulator-manipulated OTFTs are mainly enhanced by a carrier injection at the S/D regions rather than a structural ordering at the channel region.

Figure 1 shows schematic diagrams of the top-contact OTFTs with/without nanopatterns. After an aluminum (Al) layer with 70 nm thick on glass substrate was patterned for a gate electrode, a polymeric insulator of cross-linked poly(4-vilyphenol) (cPVP), formed from the solution of PVP and poly(melamine-co-formaldehyde) dissolved in propylene glycol monomethyl ether acetate, was spin-coated on the patterned Al layer and heated at 180 °C in vacuum oven. For
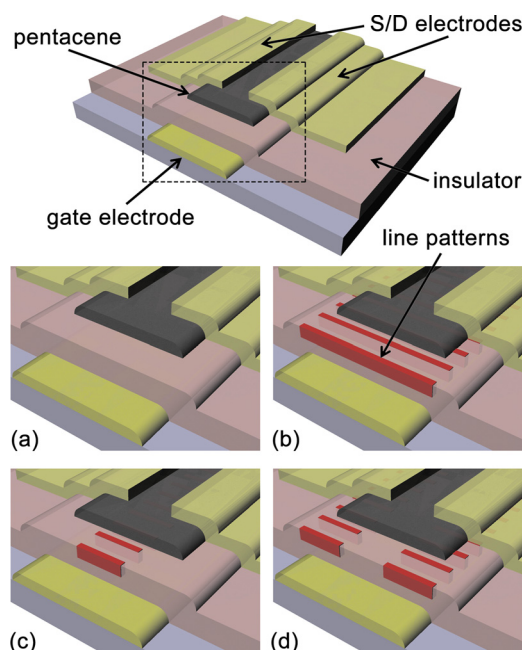

FIG. 1. (Color online) Schematic diagrams of the pentacene-based TFTs with (a) no interfacial structure and [(b)–(d)] nanoscaled line patterns between an insulating layer and a pentacene layer. The nanoscaled patterns are formed at (b) whole pentacene region, (b) channel region, and (c) S/D regions, respectively.

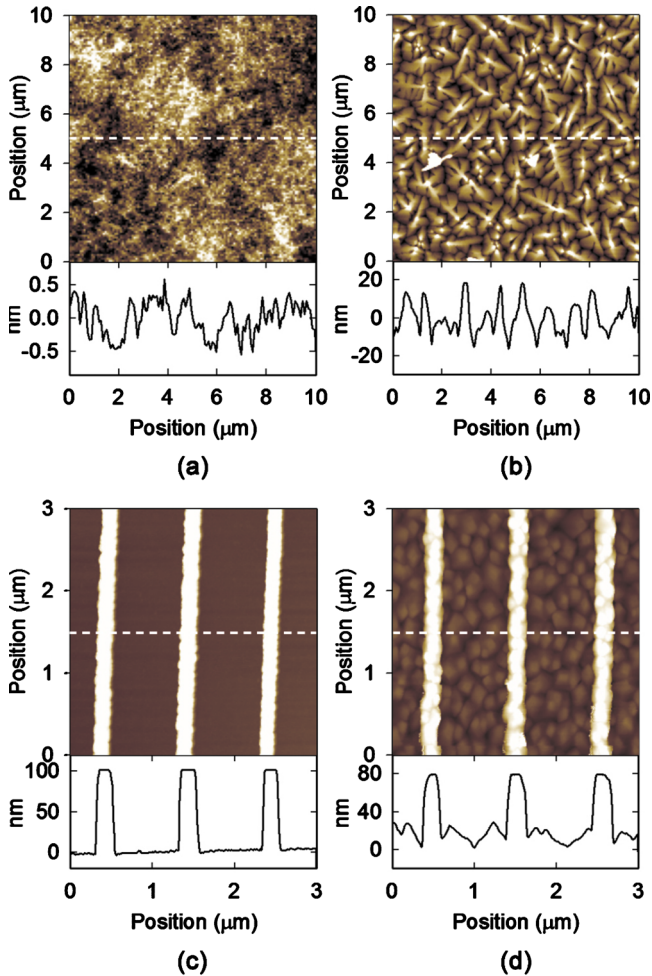a)Author to whom correspondence should be addressed. Electronic mail: jhoon@hanyang.ac.kr.

FIG. 2. (Color online) AFM images of (a) the bare cPVP layer and (b) the pentacene layer on it, and (c) the line-shaped nanopatterns on the cPVP layer and (d) the pentacene layer on it with the line patterns. The line profiles represent the surface morphologies depicted by the dashed lines in each AFM image.

the nanopatterns onto the gate insulator, the e-beam lithography using ma-N2401 photoresist (Micro Resist Technology, Germany) was carried out with Tescan MIRA-XMH scanning electron microscope equipped with Raith ELPHY Plus beam controller. The negative tone ma-N2401 photoresist was spin-coated at 4000 rpm for 30 s and dehydrated on a hotplate at 90 °C for 90 s. To investigate an effect of the selective nanopatterns on the OTFT performances, we prepared four test samples with the line-shaped nanopatterns at the channel region, S/D regions, whole region, and a reference sample without any pattern as shown in Fig. 1. The height and the width of the line-shaped patterns with the period of 1 μm were 100 nm and 200 nm, respectively. A 60-nm-thick pentacene (Tokyo Chemical Industry, Japan) layer was directly deposited under a basal pressure of about 10^{-6} Torr at an evaporation rate of 0.5 Å/s on the insulator without any further purification. Finally, top-contact gold S/D electrodes of 50 nm were deposited through a shadow mask with channel length (L) of 100 μm and width (W) of 300 μm.

Figure 2 shows the surface morphologies of the cPVP and the pentacene layers with/without the nanopatterns measured by an atomic force microscope (AFM; XE-100, Park system). As shown in Figs. 2(a) and 2(b), the smooth bare cPVP layer with a small root-mean-square value of rough-
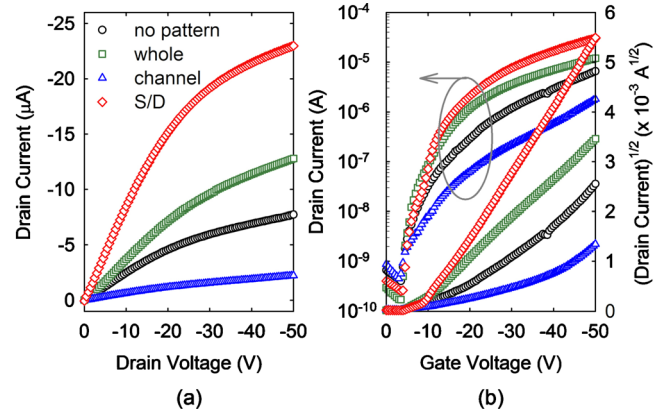

FIG. 3. (Color online) Electrical (a) transfer curves at a gate voltage of 50 V and (b) output characteristics at a drain voltage of 50 V of the pentacene-based TFTs.

ness (0.309 nm) and the typical herringbonelike growth of pentacene crystals on the cPVP were observed.[16–18] Onto the insulator layer with the good fidelity of one-dimensional (1D) line shapes in Fig. 2(c), the smaller grains of the pentacene were observed than that onto the bare cPVP as shown in Fig. 2(d). It should be noted that the grain size of the pentacene layer does not directly reflect the OTFT performances.[8,19] An anisotropy of the grains does not observed in the AFM image. As reported previously, the anisotropy of grains was introduced if we control the periodicity and size of nanogrid.[9] In our case, however, we selected the conditions which did not show anisotropy because we just focused on the effect of carrier injection with nanopatterns.

Figure 3 shows the electrical characteristics of the OTFTs with/without the selective nanopatterns. Here, the direction of the 1D nanopatterns was aligned parallel to the direction of the current flow. The device performances of each OTFT sample such as the mobility (μ_{eff}), the threshold voltage (V_T), and the on/off ratio ($I_{on/off}$) were summarized in Table I. The field effect mobilities of the nanopatterned OTFTs at the whole region and the S/D regions were enhanced than the mobility of the reference OTFT with no pattern. Especially, the mobility of the S/D-patterned OTFT was five times greater than that of the reference while the wholly patterned OTFT at both channel and S/D regions increased only about two times. It should be noted that the injection area in the nanopatterned OTFTs was just increased by 20% since the height of the line-shaped patterns with the period of 1 μm was 100 nm. More interesting point is that the mobility of the channel-patterned OTFT was rather less. We have to note that the same results were obtained for the OTFTs with the 1D nanopatterns perpendicular to the direction of the current flow. It means that the nanopatterns at the S/D regions remarkably improve the device performances, whereas those at the channel region seriously degrade them.

TABLE I. Device performances of the OTFTs at a drain voltage of 50 V.

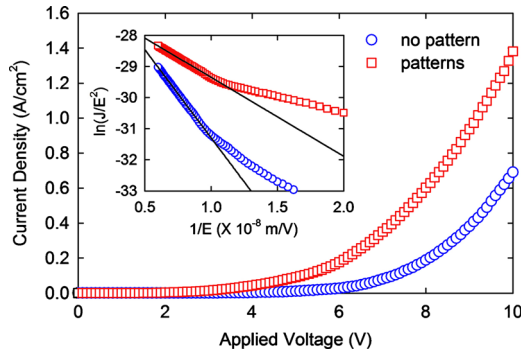| Patterned region	μ_{eff} (cm^2/V s)	V_T (V)	$I_{on/off}$
No pattern	0.153	−6.4	1.62×10^4
Whole regions	0.290	−8.1	7.01×10^4
Channel region	0.036	−6.9	0.40×10^4
S/D regions	0.798	−8.5	11.90×10^4

FIG. 4. (Color online) Current density characteristics in Au/pentacene (with/without patterns)/Au configurations. Inset represents plots of $\ln(J/E^2)$ vs $1/E$ to estimate exponents $\kappa\varphi^{3/2}$ in Eq. (1) deduced by the slopes of solid lines.

These results suggest that the mobility enhancement is mainly attributed to an increase in injection carriers at the S/D electrodes with the nanopatterns rather than carrier flow at the channel region. Moreover, the rough valleys by the nanopatterns at the channel region give rise to hinder the carrier movement,[20] and thus the carrier flow at the channel region is degraded by interface roughness scattering at the insulating layer due to the nanopatterns.[21,22]

The conducting properties in a MSM structure were measured to investigate the effect of the nanopatterns at the S/D regions on the carrier injection. The MSM samples were prepared with a sequential deposition of the bottom gold, the pentacene (60 nm thick) with/without the nanopatterns, and the top gold. In these pentacene-based devices, the hole is a dominant carrier and the injection current density (J), which is mainly attributed to a tunneling process at high field regime, strongly depends on the energy barrier between the gold and the pentacene thin layers. From the FN tunneling theory given as[15]

$$J \propto E^2 \exp\left(\frac{-\kappa\varphi^{3/2}}{E}\right), \qquad (1)$$

we could estimate the injection barrier for both MSM samples with/without the nanopatterns. Here, E, φ, and κ are an electric field strength, an injection barrier height, and a FN constant depending on an effective mass of hole, respectively. Figure 4 shows the current density characteristics of the MSM samples and inset represents plots of $\ln(J/E^2)$ versus $1/E$ to estimate the injection barriers. In the plot of $\ln(J/E^2)$ versus $1/E$, the slope of the straight line at high field regime corresponds the exponent $\kappa\varphi^{3/2}$ in Eq. (1). The slopes of the straight lines doing a least-square fit to Eq. (1) for the bare and the nanopatterned MSM samples were -5.68×10^8 and -2.53×10^8, respectively. Using the effective mass of hole (1.46×10^{-30} kg),[23] the injection barriers of the bare and the nanopatterned samples were calculated to be 0.16 eV and 0.10 eV, respectively.[24] The nanopatterns at the S/D regions form the metal clusters at the interface between metal and insulator such that these metal clusters effectively impede metal diffusion into the bulk and reduce the injection barrier in the tunneling process.[13] As a result, the lower barrier gives rise to improvement of the hole injection by the tunneling process and thus the device performances of the OTFT are significantly enhanced.

In conclusion, we investigated the effect of the nanopatterns on the performances of the top contact OTFTs through the selective patterns onto the insulating layer. Using the e-beam lithography, the 1D nanopatterns were selectively formed at the channel region and/or the S/D regions. The performance of the S/D-patterned OTFT was greater than that of the reference OTFT without the nanopattern while the performance of the channel-patterned OTFT was rather less. From the FN analysis of the current characteristics in the MSM structure, the nanopatterns at the S/D regions were expected to impede metal diffusion into the bulk and contribute to the reduction in the injection barrier. However, the nanopatterns at the channel region were expected to generate the interface roughness scattering and thus the performances were degraded. As a result, the device performance of the OTFTs with the nanopatterns strongly depends on a carrier injection at the S/D regions rather than a carrier flow at the channel region. We believe that there is the optimum conditions of nanopatterns to enhance both carrier injection and molecular ordering, and the study is now under progressing.

[1] F. Garnier, R. Hajlaoui, A. Yassar, and P. Srivastava, Science **265**, 1684 (1994).
[2] S. R. Forrest, Nature (London) **428**, 911 (2004).
[3] R. Rotzoll, S. Mohapatra, V. Olariu, R. Wenz, M. Grigas, K. Dimmler, O. Shchekin, and A. Dodabalapur, Appl. Phys. Lett. **88**, 123502 (2006).
[4] L. Zhou, A. Wanga, S.-C. Wu, J. Sun, S. Park, and T. N. Jackson, Appl. Phys. Lett. **88**, 083502 (2006).
[5] M. Mizukami, N. Hirohata, T. Iseki, K. Ohtawara, T. Tada, S. Yagyu, T. Abe, T. Suzuki, Y. Fujisaki, Y. Inoue, S. Tokito, and T. Kurita, IEEE Electron Device Lett. **27**, 249 (2006).
[6] M. Lefenfeld, G. Blanchet, and J. A. Rogers, Adv. Mater. (Weinheim, Ger.) **15**, 1188 (2003).
[7] W.-Y. Chou and H.-L. Cheng, Adv. Funct. Mater. **14**, 811 (2004).
[8] J.-H. Bae, W.-H. Kim, H. Kim, C. Lee, and S.-D. Lee, J. Appl. Phys. **102**, 063508 (2007).
[9] S. J. Jo, C. S. Kim, M. J. Lee, J. B. Kim, S. Y. Ryu, J. H. Noh, K. Ihm, H. K. Baik, and Y. S. Kim, Adv. Mater. (Weinheim, Ger.) **20**, 1146 (2008).
[10] W.-K. Kim and J.-L. Lee, Appl. Phys. Lett. **88**, 262102 (2006).
[11] X. Yan, J. Wang, H. Wang, H. Wang, and D. Yan, Appl. Phys. Lett. **89**, 053510 (2006).
[12] T. Maeda, H. Kato, and H. Kawakami, Appl. Phys. Lett. **89**, 123508 (2006).
[13] J.-H. Bae, W.-H. Kim, C.-J. Yu, and S.-D. Lee, Jpn. J. Appl. Phys. **48**, 020209 (2009).
[14] Q. Sun, J.-H. Kim, J.-H. Park, and S. Seo, Appl. Phys. Lett. **96**, 103301 (2010).
[15] R. H. Fowler and L. Nordheim, Proc. R. Soc. London, Ser. A **119**, 173 (1928).
[16] S. Y. Park, M. Park, and H. H. Lee, Appl. Phys. Lett. **85**, 2283 (2004).
[17] S. Y. Yang, K. Shin, and C. E. Park, Adv. Funct. Mater. **15**, 1806 (2005).
[18] S. E. Fritz, T. W. Kelly, and C. D. Frisbie, J. Phys. Chem. B **109**, 10574 (2005).
[19] E. M. Muller and J. A. Marohn, Adv. Mater. (Weinheim, Ger.) **17**, 1410 (2005).
[20] S. Steudel, S. D. Vusser, S. D. Jonge, D. Janssen, S. Verlaak, J. Genoe, and P. Heremans, Appl. Phys. Lett. **85**, 4400 (2004).
[21] H.-S. Seo, Y.-S. Jang, Y. Zhang, P. Syed Abthagir, and J. H. Choi, Org. Electron. **9**, 432 (2008).
[22] S. Okur, F. Yakuphanoglu, and E. Stathatos, Microelectron. Eng. **87**, 635 (2010).
[23] N. Nakamura, N. Goto, N. Ohashi, M. Sakai, and K. Kudo, Appl. Phys. Lett. **86**, 122112 (2005).
[24] J. Park and J. S. Choi, Synth. Met. **155**, 657 (2005).